Cylindrical Fresnel lenses based on carbon nanotube forests

Haider Butt, Ranjith Rajesekharan, Qing Dai, Sohab Sarfraz, R. Vasant Kumar et al.

Cylindrical Fresnel lenses based on carbon nanotube forests

Haider Butt,[1,a)] Ranjith Rajesekharan,[2] Qing Dai,[1] Sohab Sarfraz,[3] R. Vasant Kumar,[3] Gehan A. J. Amaratunga,[1,4] and Timothy D. Wilkinson[1]
[1]*Electrical Engineering Division, Department of Engineering, University of Cambridge, Cambridge CB3 0FA, United Kingdom*
[2]*School of Physics, University of Melbourne, Melbourne, Victoria 3010, Australia*
[3]*Department of Materials Science & Metallurgy, University of Cambridge, Cambridge, United Kingdom*
[4]*Sri Lanka Institute of Nanotechnology (SLINTEC), Lot 14, Zone A, EPZ, Biyagama, Sri Lanka*

(Received 3 August 2012; accepted 28 November 2012; published online 12 December 2012)

The forests of carbon nanotubes have been termed as the darkest man-made materials. Such materials exhibit near-perfect optical absorption (reflectance $\sim 0.045\%$) due to low reflectance and nanoscale surface roughness. We have demonstrated the utilization of these perfectly absorbing forests to produce binary amplitude cylindrical Fresnel lenses. The opaque Fresnel zones are defined by the dark nanotube forests and these lenses display efficient focusing performance at optical wavelengths. Lensing performance was analyzed both computationally and experimentally with good agreement. Such nanostructure based lenses have many potential applications in devices like photovoltaic solar cells. © *2012 American Institute of Physics*. [http://dx.doi.org/10.1063/1.4772002]

Carbon nanotubes (CNTs) have been the focus of a large amount of research during recent years.[1,2] Their optical properties have been thoroughly studied and a myriad of interesting photonic applications reported.[3,4] Due to advancements in nanofabrication techniques, highly controlled growth of carbon nanotubes is now possible.[5] The precise arrangement and pattern of the carbon nanotubes in these arrays is one of the key features that control the optical properties achieved. When CNT arrays are fabricated with average interspacing smaller than the wavelength of light, they display effectively different index of refraction and surface roughness.[6] In such an arrangement, these arrays act as effective composites of air and nanotubes displaying specifically engineered optical properties.[7]

Recently, Yang *et al.* reported that the forests of vertically aligned carbon nanotubes have the capacity to absorb 99.955% of incident visible light and were termed as the darkest man-made materials.[8] The CNTs were grown at subwavelength spacings. As the average spacing between the nanotubes was much smaller than the wavelength of the light, the optical properties of the carbon nanotube forest could be formulated using effective medium theory and the material can be regarded as a composite with an effective index of refraction.[9] The refractive index and absorption coefficient can be calculated with the assumption that each nanotube has the dielectric function of graphite.[8] Such CNT forests produce a near-perfect optical absorption material (reflectance $\sim 0.045\%$) due to an extremely low reflectance and nanoscale surface roughness.[10] With an index of refraction very close to air, most of the incident light propagates into the nanotube forests. The light is then absorbed and scattered by the carbon nanotubes, due to their large imaginary refractive index component in the visible.[11] We present the use of carbon nanotube forests as a perfect absorbing composite to produce a cylindrical Fresnel lens.

Fresnel lenses[12] are widely used in the optical industry and are key elements in systems like integrated optics,[13,14] optical interconnects,[15] beam focusing,[16,17] and maskless lithography systems.[18] Fresnel lenses require a flat surface rather than a curved shape, which makes mounting much more straight forward and increases the tolerance to surface errors.[19] These lenses usually consist of alternating transparent and opaque zones, with respect to the incident light.[13] One of the main problems Fresnel lenses suffer from is reflections from the opaque zones and a corresponding degradation in focusing and lensing properties. In our previous work,[20] we proposed a solution to this by using random arrays (forests)[21] of vertically aligned carbon nanotubes as the opaque zones in circular Fresnel lenses. Opaque regions defined by the CNTs forests display near perfect absorption with high contrast and focusing capabilities.

Here, we present CNT forest based Fresnel lenses with a cylindrical geometry which allows them to be fabricated over large areas. By utilizing inexpensive photolithographic patterning techniques, large area fabrication of these binary amplitude cylindrical Fresnel lenses is possible. Cylindrical Fresnel lenses encompassing a large area have enormous potential for use as concentrators in photodiodes and other photovoltaic applications.[22]

A cylindrical Fresnel lens consists of a plate with alternating transparent and opaque zones (Figure 1(a)) having a distance from the central axis proportional to the square root of integer multiples of the operating wavelength.[23] As a result of this, at a certain distance on the central plane (perpendicular to the lens), the optical path lengths of the diffracted beams differ by an integral number of wavelengths, and constructive interference occurs creating a focus point.

A CNT forest based Fresnel lens has been designed to operate in the optical regime. The focal length f of the lens is related to the distance d of successive Fresnel zone edges from the central axis by $d^2 = fn\lambda$. Setting the focal length and optical wavelength to 125 μm and 800 nm, the spacings and widths of the Fresnel zones were calculated for different values

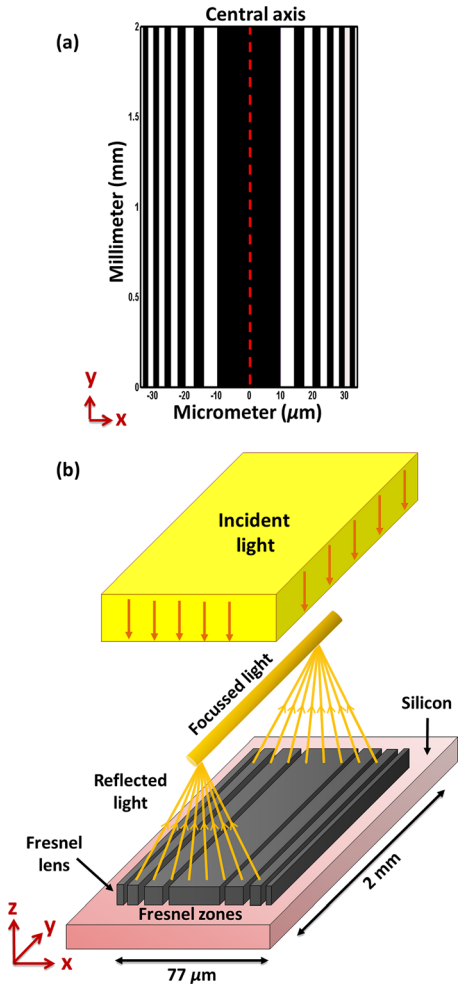

FIG. 1. (a) Calculated geometry of carbon nanotube based cylindrical Fresnel lens having a design focal length of 125 μm at $\lambda = 800$ nm. The lens measured 77 μm by 2 mm. (b) Schematic showing the geometry and reflection mode operation of the Fresnel lens, incident light form the top.

of $n = 1, 2, 3, \ldots$. Figure 1(a) shows the calculated Fresnel lens, having a width of 77 μm (x direction) and extending over a length of 2 mm (y direction). As the area of all the Fresnel zones is equal, the zones close to the central axis are widely spaced. As the distance from the central axis increases, the zone spacing decreases. The lens was designed for an operating wavelength λ of 800 nm; however, it was simulated and later characterised at different optical frequencies. This changes the effective focal length of the lens, in accordance with the equation $f = d^2/n\lambda$. Figure 1(b) shows the three-dimensional (3D) schematic diagram of the Fresnel lens geometry and its operation. Due to the fabrication on a silicon substrate, the lens operated in the reflection mode. The incident light was reflected off the silicon substrate within the non-forest covered Fresnel zones and was then focused at the focal plane.

The nanotube based Fresnel lens was modeled using finite element method (FEM) to analyze the wave propagation from it and focusing performance. For the purpose of simplicity and to utilize the cylindrical symmetry of the lens, a two-dimensional (2D) model was established depicting the cross-section of the Fresnel lens, as shown in Figure 2. The opaque zones comprising CNT forests were modeled as periodic arrays of CNTs with a subwavelength radius and spacing of 50 nm and 250 nm, respectively. The CNT forests comprise

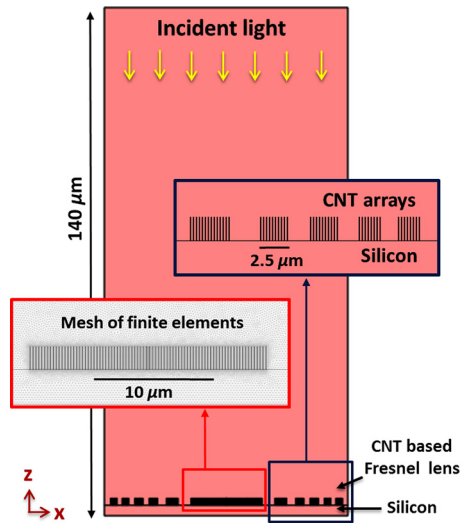

FIG. 2. 2D cross-sectional geometry of the simulated CNT based Fresnel lens on silicon. Opaque zones are represented by the CNT arrays and the lens operated in reflection mode. Insets show the CNT arrays and mesh elements utilized to resolve the computational domain.

randomly placed nanotubes with spacings of the order of a few tens of nanometers. It is a difficult computational task to model such random arrays in most commercially available simulation software packages, due to the small sized mesh elements required. For this reason, a densely periodic CNT array was used, the geometry of which was simpler to construct. A plane wave was normally incident on the lens and its focusing was simulated in the reflection mode. To simulate the wave propagation a scalar equation was solved for the transverse electric field component E across the computation domain, $-\nabla \cdot \nabla E - n^2 k_0^2 E = 0$, where n is the refractive index and k_0 is the free-space wave number.

Modeling of CNT based lens was computationally intensive due to the huge contrast between the dimensions of the CNTs and the overall Fresnel lens. The carbon nanotube radius was about 50 nm while the Fresnel lens was designed with a width of 77 μm. Designed focal length of 125 μm meant that the model geometry had to be at least 80 μm wide and 140 μm in length (Figure 2) to simulate the focusing properly. The FEM simulation method divides the computational domain (model geometry) into smaller finite elements to produce a mesh. To effectively model the nanotubes in the model geometry, finite elements with sizes varying from 10 to 200 nm were used. Small sized (10 nm) and high density finite elements were declared around the CNTs to resolve them accurately in the simulation, as shown in the inset of Figure 2. Additionally, a maximum finite element size of 200 nm was chosen, to avoid wave propagation computation errors incurred when the mesh element size is bigger than at least $\lambda/4$ (for $\lambda = 850$ nm). Hence, to simulate wave propagation of wavelengths smaller than 850 nm, fairly higher computational memory and time are required.

Light propagation across the Fresnel lens was simulated for a wavelength of 850 nm in reflection mode and strong focusing was observed. As presented in the intensity plot of Figures 3(a) and 3(b), the incident light (from the top) on the lens is mostly blocked by the carbon nanotube arrays and reflection only occurs from silicon through the gaps

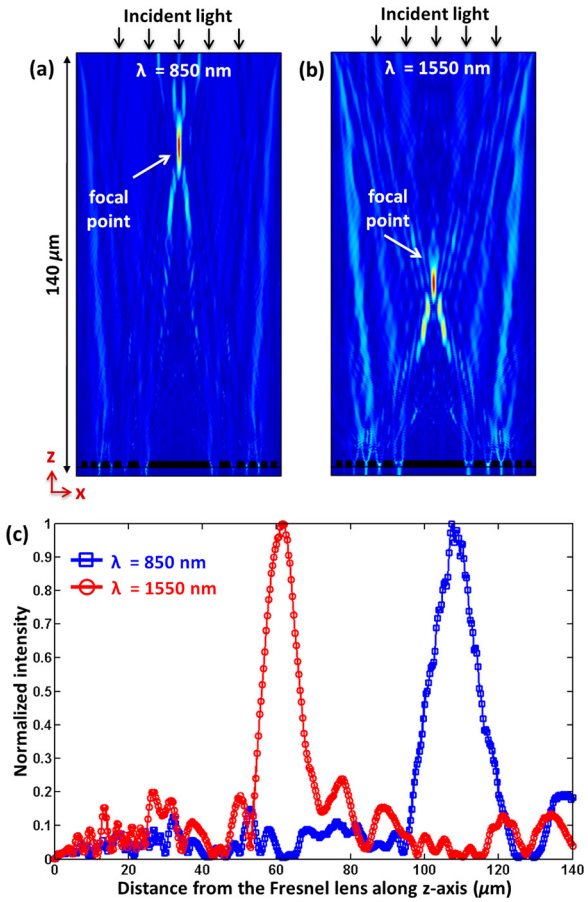

FIG. 3. Simulated wave propagation (intensity) of (a) 850 nm and (b) 1550 nm waves across the Fresnel lens. The reflected light is focused into the focus plane. (c) Intensity plots with distance extending from the lens center to the focal plane. The focal lengths decrease with increasing λ.

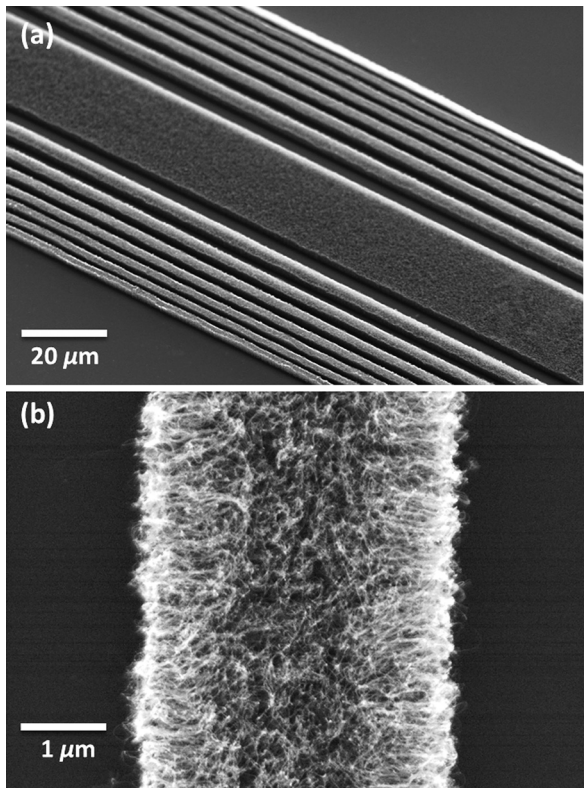

FIG. 4. (a) SEM image of cylindrical Fresnel lens based on the carbon nanotube forests, fabricated on a silicon substrate. (b) Higher magnification image showing the CNT forest in an opaque Fresnel zone.

(transparent Fresnel zones). Due to the path length differences between the gaps, a strong focus spot is produced at a distance of about 110 μm from the lens. The intensity profile plotted across the distance from the centre of the lens to the focal plane illustrates the focal length (Figure 3(c)). The simulation results confirm that each CNT array acts as an opaque zone to produce a cylindrical Fresnel lenses.

To study the focusing response of the lens with incident light of different wavelengths, the wave propagation was also simulated for a wavelength of 1550 nm. As shown in Figure 3(b), the lens presented strong focusing of the 1550 nm wavelength as well as a shorter focal length of 60 μm (Figure 3(c)). As expected the focal length decreased with the increase in wavelength, which is in agreement with the equation $f = d^2/n\lambda$ used to design the Fresnel lens.

Based on these simulation results, a CNT forest based cylindrical Fresnel lens was fabricated using photolithography and chemical vapour deposition (CVD). A silicon substrate was patterned by photolithography with the designed Fresnel zones, in which an Al 10 nm/Fe 1 nm multilayer catalyst was deposited by sputtering. Then, thermal CVD was employed to grow strips of vertically aligned carbon nanotube forests. First, the sample was annealed in argon at 420 °C for 30 s to form catalyst nano-particles. Then, CVD was carried out at a growth temperature of 520 °C and pressure of 10 mbar with a flow rate of 200 SCCM of acetylene (C_2H_2), which gave a carbon nanotube forest length of 12 μm after 60 s growth. Scanning electron microscope (SEM) images of the fabricated Fresnel lens are shown in Figure 4. Very uniform CNT forests were fabricated in the opaque Fresnel zones. Each lens was 77 μm wide and 2 mm in length, consisting of 15 rows of CNT forests. These lenses can be fabricated over larger areas by patterning bigger substrates using photolithography.

The fabricated CNT Fresnel lens array was characterised under an optical microscope (Olympus −300) at a magnification of ×20. Figure 5(a) shows two lenses under the microscope. It can be observed that the carbon nanotube forest based composite acted as near perfect optical absorber producing opaque Fresnel zones. The incident light from the microscope is only reflected from the silicon substrate constituting reflective Fresnel zones. Figure 5(b) shows the cylindrical lenses focusing light. Light is focussed in the form of a line in the focal plane. To observe the focusing more clearly, a 2D intensity plot for the red region of the optical spectrum was acquired across the focal plane of the two lenses (Figure 5(c)). Rows of high contract and uniform focused light were clearly observed in the centre of the Fresnel lenses.

The focal length was experimentally measured as 156 μm which was the equivalent focal length for the red wavelength (635 nm) and in excellent agreement with the theoretical results predicted by the equation $f = d^2/n\lambda$. The slight variation in the value was because of fabrication tolerances. Figure 5(d) shows the light intensity profile across the focal plane. The intensity profile shows that the Fresnel lenses performed well-defined focusing with good contrast.

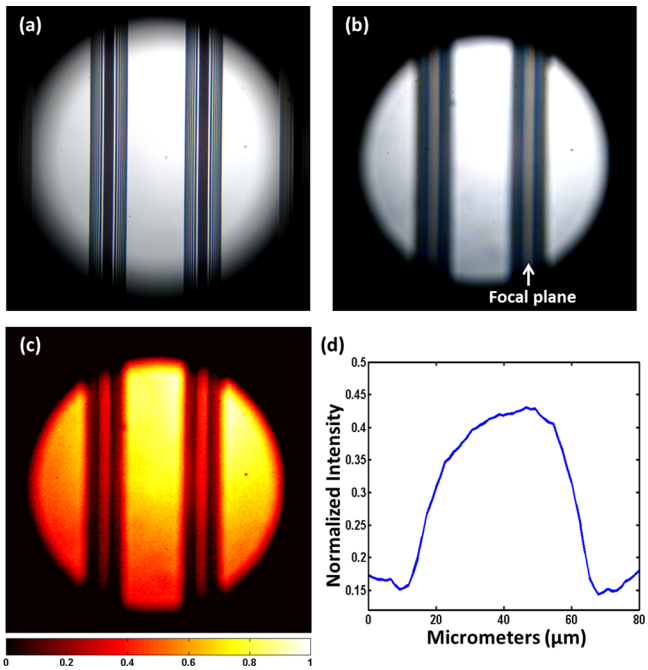

FIG. 5. (a) CNT based cylindrical Fresnel lenses under an optical microscope. Each lens having 15 opaque zones extended to an area of width 77 μm and length 2 mm. (b) Fresnel lenses showing the focusing of light in the focal plane. (c) 2D intensity plot across the focal plane. Focused rows of light are observed in the middle of the lenses. (d) Light intensity plot across the Fresnel lens showing focusing.

The lens efficiency was measured from the ratio of light intensity at the focal point to the total light intensity falling on lens. An efficiency of the order of 15% was calculated for the red region of the optical spectrum. The lens array was fabricated on a silicon substrate (reflectivity 40%) and half of the lens area was covered by CNT forest. The efficiency can be improved by coating the reflecting zones with a metal such as Al. In future, these lenses can also be fabricated using transparent nanomaterials like zinc oxide nanowires and graphene. This will improve the lens efficiency and device application as concentrators in solar cells and other photovoltaic devices.

In conclusion, we have demonstrated a reflective cylindrical Fresnel lenses based on forests of carbon nanotubes grown on silicon. These forests display exceptional absorption capacities and are perfect materials for producing opaque zones in the Fresnel lens. Through calculation and FEM computational simulations, the lens was designed to operate in the optical regime. The lens fabrication was performed using an inexpensive technique of photolithography to perform large area fabrication of these lenses. Focusing properties of the Fresnel lenses were experimentally characterized using an optical microscope. High contrast and continuous focusing for light was observed in the focal plane of each lens.

[1]S. Iijima, Nature **354**, 56–58 (1991).
[2]R. H. Baughman, A. A. Zakhidov, and W. A. de Heer, Science **297**, 787–792 (2002).
[3]K. Kempa, B. Kimball, J. Rybczynski, Z. P. Huang, P. F. Wu, D. Steeves, M. Sennett, M. Giersig, D. V. G. L. N. Rao, D. L. Carnahan, D. Z. Wang, J. Y. Lao, W. Z. Li, and Z. F. Ren, Nano Lett. **3**, 13–18 (2003).
[4]H. Butt, Q. Dai, P. Farah, T. Butler, T. D. Wilkinson, J. J. Baumberg, and G. A. J. Amaratunga, Appl. Phys. Lett. **97**, 163102-3 (2010).
[5]K. B. K. Teo, M. Chhowalla, G. A. J. Amaratunga, W. I. Milne, D. G. Hasko, G. Pirio, P. Legagneux, F. Wyczisk, and D. Pribat, Appl. Phys. Lett. **79**, 1534–1536 (2001).
[6]H. Butt, Q. Dai, R. Rajesekharan, T. D. Wilkinson, and G. A. J. Amaratunga, ACS Nano **5**, 9138–9143 (2011).
[7]D. R. Smith, J. B. Pendry, and M. C. K. Wiltshire, Science **305**, 788–792 (2004).
[8]Z.-P. Yang, L. Ci, J. A. Bur, S.-Y. Lin, and P. M. Ajayan, Nano Lett. **8**, 446–451 (2008).
[9]F. J. Garcia-Vidal, Nat. Photonics **2**, 215–216 (2008).
[10]T. d. l. Arcos, P. Oelhafen, and D. Mathys, Nanotechnology **18**, 265706 (2007).
[11]E. Lidorikis and A. C. Ferrari, ACS Nano **3**, 1238–1248 (2009).
[12]B. A. Anicin, V. M. Babovic, and D. M. Davidovic, Am. J. Phys. **57**, 312–316 (1989).
[13]K. Rastani, A. Marrakchi, S. F. Habiby, W. M. Hubbard, H. Gilchrist, and R. E. Nahory, Appl. Opt. **30**, 1347–1354 (1991).
[14]K. Kodate, E. Tokunaga, Y. Tatuno, J. Chen, and T. Kamiya, Appl. Opt. **29**, 5115–5119 (1990).
[15]M. Ferstl and A.-M. Frisch, J. Mod. Opt. **43**, 1451–1462 (1996).
[16]F. Mahmoud, J. K. Keith, P. Scott, O. Nordman, and P. Nasser, Opt. Eng. **37**, 1169–1174 (1998).
[17]B. Morgan, C. M. Waits, J. Krizmanic, and R. Ghodssi, J. Microelectromech. Syst. **13**, 113–120 (2004).
[18]D. J. D. Carter, D. Gil, R. Menon, M. K. Mondol, H. I. Smith, and E. H. Anderson, J. Vac. Sci. Technol. B **17**, 3449–3452 (1999).
[19]I. M. Barton, J. A. Britten, S. N. Dixit, L. J. Summers, I. M. Thomas, M. C. Rushford, K. Lu, R. A. Hyde, and M. D. Perry, Appl. Opt. **40**, 447–451 (2001).
[20]R. Rajasekharan, H. Butt, Q. Dai, T. D. Wilkinson, and G. A. J. Amaratunga, Adv. Mater. **24**, OP170–OP173 (2012).
[21]K. K. S. Lau, J. Bico, K. B. K. Teo, M. Chhowalla, G. A. J. Amaratunga, W. I. Milne, G. H. McKinley, and K. K. Gleason, Nano Lett. **3**, 1701–1705 (2003).
[22]W. T. Xie, Y. J. Dai, R. Z. Wang, and K. Sumathy, Renewable Sustainable Energy Rev. **15**, 2588–2606 (2011).
[23]G. Saxby, *Practical Holography*, 3rd ed. (IOP/CRC, UK, 2004).